

SOME APPROXIMATE BUCKLING SOLUTIONS OF TRIPLE-WALLED CARBON NANOTUBE

V. Senthilkumar^{1,*} 

¹CSIR Fourth Paradigm Institute (Erstwhile CSIR Centre for Mathematical Modelling and Computer Simulation), Belur Campus, Bangalore-560037, Karnataka, India

*E-mail: senthil@csir4pi.in

Received: 07 April 2022 / Published online: 16 July 2022

Abstract. The present investigation analyses the critical buckling studies of triple-walled carbon nanotube using the Euler–Bernoulli model. The present study deals with three different boundary conditions, namely, simply-simply, clamped-clamped, and clamped-simply supported carbon nanotube. Using Bubnov–Galerkin and Petrov–Galerkin methods, the continuum model estimates the critical buckling load. The main advantage of these two approximate methods is to obtain a quick and valid result. The first and second Euler critical buckling loads decrease with the increase of length to outer diameter ratio for boundary conditions like simply-simply, clamped-clamped, and clamped-simply supported. Interestingly, the increase in the length to outer diameter ratio results in the rise in third Euler critical buckling for all three different boundary conditions. These two approximate methods provide reliable buckling load estimation using suitable polynomials.

Keywords: triple-walled carbon nanotube, Bubnov–Galerkin method, Petrov–Galerkin method, buckling load.

1. INTRODUCTION

In 1991, Iijima [1] experimentally showed the carbon nanotube structure. Since then, carbon nanotubes become popular among researchers to explore the mechanical, structural [2], and electrical properties [3,4]. Buckling [5,6] of structural members plays a crucial role in understanding the elastic and inelastic behavior of the bar, beam, plate, and shell. Batra and Sears [7] used continuum models to analyze the multi-walled carbon nanostructures. The molecular simulations [8,9] provide reliable results in predicting the mechanical/structural behaviors of nanostructures. But due to the substantial computational cost required to carry out the simulations using supercomputers, the continuum models serve as an alternative approach. Elishakoff and Pentaras [10] investigated the buckling analysis of double-walled carbon nanotube using three different boundary conditions, namely simply-simply, clamped-clamped, and clamped-hinged support using Bubnov–Galerkin and Petrov–Galerkin methods. Kitipornchai et al. [11] investigated the

buckling studies of triple-walled carbon nanotube with elastic medium using polar coordinates model. Guo et al. [12] studied the critical strain behavior of carbon nanotubes using an atomic-scale finite element approach. Lu et al. [13] studied the effect of the slenderness ratio in the buckling analysis of multi-walled carbon nanotubes. Rahmani and Antonov [14] used the polar coordinates model for the buckling studies of single and multi-walled carbon nanotubes by using the finite element approach. Coşkun [15] computed the buckling loads of columns using various numerical methods. Pentaras and Elishakoff [16] estimated the vibrational frequencies for triple-walled nanotube using Euler–Bernoulli’s continuum model. In their research investigation, the estimation of frequencies happens using approximate methods like Bubnov–Galerkin and Petrov–Galerkin method in a reliable manner.

Ru [17] investigated the critical buckling study of multi-walled carbon nanotube using the van der Waals force effect. Later, Ru [18] studied the axial buckling effect of double-walled carbon nanotubes. Further, Ru [19] examined the influence of elastic medium support over critical buckling in the double-walled carbon nanotubes. Senthilkumar [20] used a semi-analytical method to study the single-walled carbon nanotube using Euler–Bernoulli’s model with nonlocal effects. Recently, Malikan et al. [21] investigated the buckling behavior of non-concentric double-walled carbon nanotubes. It is often easy to model the simply-simply supported boundary conditions because the analytical solutions are readily available. But other boundary conditions like clamped-clamped, clamped-simply supported require numerical solutions for the buckling solutions of triple-walled carbon nanotube. Elishakoff et al. [22] proposed the polynomials to estimate critical buckling loads of double-walled carbon nanotubes for simply-simply, clamped-clamped and clamped-simply supported boundary conditions using Bubnov–Galerkin and Petrov–Galerkin methods. The present investigation extends it to triple-walled carbon nanotubes. As per the author’s knowledge, the buckling studies of triple-walled carbon nanotube with the Euler–Bernoulli model for different boundary conditions are not available in the literature. This work aims to fill this void using quick and reliable numerical solutions.

2. MATHEMATICAL MODEL OF TRIPLE-WALLED NANOTUBE

Elishakoff and Pentaras [10,23] proposed the governing equations of double-walled carbon nanotube with buckling behaviour using $\sigma_{x2}^E \equiv P^E/(A_1 + A_2)$. In the present study, the buckling behaviour of third nanotube induced by considering the stress as $\sigma_{x3}^E \equiv P^E/(A_1 + A_2 + A_3)$. So the mathematical model for triple-walled carbon nanotube with buckling behaviour can be expressed as,

$$EI_1 \frac{\partial^4 w_1}{\partial x^4} + P^E \frac{A_1}{A_{T3}} \frac{\partial^2 w_1}{\partial x^2} = c_{12}(w_2 - w_1), \quad (1)$$

$$EI_2 \frac{\partial^4 w_2}{\partial x^4} + P^E \frac{A_2}{A_{T3}} \frac{\partial^2 w_2}{\partial x^2} = c_{23}(w_3 - w_2) - c_{12}(w_2 - w_1), \quad (2)$$

$$EI_3 \frac{\partial^4 w_3}{\partial x^4} + P^E \frac{A_3}{A_{T3}} \frac{\partial^2 w_3}{\partial x^2} = -c_{23}(w_3 - w_2), \quad (3)$$

where w_1 , w_2 , and w_3 are the transverse displacements of the innermost carbon nanotube, middle carbon nanotube, and outer carbon nanotube, respectively. I_1 , I_2 , and I_3 are the moment of inertia of the innermost carbon nanotube, middle carbon nanotube, and outer carbon nanotubes. A_1 , A_2 , and A_3 are the innermost carbon nanotube, middle carbon nanotube, and outer carbon nanotubes' cross-sectional area. E , P^E , L , c_{12} , and c_{23} are Young's modulus, Euler's buckling load of triple-walled carbon nanotube, length of the nanotube, and the van der Waals interaction coefficients. Here A_{T3} is defined as $A_{T3} = (A_1 + A_2 + A_3)$. It is interesting to note that when $c_{23} = 0$, $A_3 = 0$, $I_3 = 0$, and $w_3 = 0$, the present model leads to the buckling model of Elishakoff and Pentaras [10] for the double-walled carbon nanotube. Using a non-dimensional approach, the governing equation of triple-walled carbon nanotube takes form as,

$$\frac{d^4 \bar{W}_1}{d\bar{X}^4} = \beta_1 (\bar{W}_2 - \bar{W}_1) - (\alpha_{twn}^E) \frac{d^2 \bar{W}_1}{d\bar{X}^2}, \quad (4)$$

$$\frac{d^4 \bar{W}_2}{d\bar{X}^4} = \beta_2 (\bar{W}_3 - \bar{W}_2) + \left(\frac{\beta_1}{\delta_1} \right) (\bar{W}_1 - \bar{W}_2) - (\alpha_{twn}^E) \left(\frac{\varepsilon_1}{\delta_1} \right) \frac{d^2 \bar{W}_2}{d\bar{X}^2}, \quad (5)$$

$$\frac{d^4 \bar{W}_3}{d\bar{X}^4} = \beta_2 \left(\frac{\delta_1}{\delta_2} \right) (\bar{W}_2 - \bar{W}_3) - (\alpha_{twn}^E) \left(\frac{\varepsilon_2}{\delta_2} \right) \frac{d^2 \bar{W}_3}{d\bar{X}^2}, \quad (6)$$

where

$$w_1(\bar{X}, t) = \bar{W}_1(\bar{X}) e^{i\omega_{twn} t}, \quad w_2(\bar{X}, t) = \bar{W}_2(\bar{X}) e^{i\omega_{twn} t}, \quad (7)$$

$$w_3(\bar{X}, t) = \bar{W}_3(\bar{X}) e^{i\omega_{twn} t}, \quad \bar{X} = \frac{x}{L}, \quad (8)$$

$$\alpha_{twn}^E = \frac{P^E A_1 L^2}{EI_1 (A_1 + A_2 + A_3)}, \quad \beta_1 = \frac{c_{12} L^4}{EI_1}, \quad \beta_2 = \frac{c_{23} L^4}{EI_2}, \quad (9)$$

$$\varepsilon_1 = \frac{A_2}{A_1}, \quad \varepsilon_2 = \frac{A_3}{A_1}, \quad \delta_1 = \frac{I_2}{I_1}, \quad \delta_2 = \frac{I_3}{I_1}. \quad (10)$$

3. SIMPLY-SIMPLY SUPPORTED

For the triple-walled carbon nanotube with simply-simply supported boundary conditions at both ends, the non-dimensional form converts as,

$$\bar{W}_1 \Big|_{\bar{X}=0} = 0, \quad \frac{d^2 \bar{W}_1}{d\bar{X}^2} \Big|_{\bar{X}=0} = 0, \quad \bar{W}_2 \Big|_{\bar{X}=0} = 0, \quad (11)$$

$$\frac{d^2 \bar{W}_2}{d\bar{X}^2} \Big|_{\bar{X}=0} = 0, \quad \bar{W}_3 \Big|_{\bar{X}=0} = 0, \quad \frac{d^2 \bar{W}_3}{d\bar{X}^2} \Big|_{\bar{X}=0} = 0, \quad (12)$$

$$\bar{W}_1 \Big|_{\bar{X}=1} = 0, \quad \frac{d^2 \bar{W}_1}{d\bar{X}^2} \Big|_{\bar{X}=1} = 0, \quad \bar{W}_2 \Big|_{\bar{X}=1} = 0, \quad (13)$$

$$\frac{d^2 \bar{W}_2}{d\bar{X}^2} \Big|_{\bar{X}=1} = 0, \quad \bar{W}_3 \Big|_{\bar{X}=1} = 0, \quad \frac{d^2 \bar{W}_3}{d\bar{X}^2} \Big|_{\bar{X}=1} = 0. \quad (14)$$

By ignoring the third nanotube's effect as $w_3 = 0$, the present boundary conditions convert to double-walled nanotube's criteria [23].

4. CLAMPED-CLAMPED SUPPORTED

The non-dimensional form of clamped-clamped boundary conditions at both ends for triple-walled carbon nanotube is,

$$\bar{W}_1 \Big|_{\bar{X}=0} = 0, \quad \frac{d\bar{W}_1}{d\bar{X}} \Big|_{\bar{X}=0} = 0, \quad \bar{W}_2 \Big|_{\bar{X}=0} = 0, \quad (15)$$

$$\frac{d\bar{W}_2}{d\bar{X}} \Big|_{\bar{X}=0} = 0, \quad \bar{W}_3 \Big|_{\bar{X}=0} = 0, \quad \frac{d\bar{W}_3}{d\bar{X}} \Big|_{\bar{X}=0} = 0, \quad (16)$$

$$\bar{W}_1 \Big|_{\bar{X}=1} = 0, \quad \frac{d\bar{W}_1}{d\bar{X}} \Big|_{\bar{X}=1} = 0, \quad \bar{W}_2 \Big|_{\bar{X}=1} = 0, \quad (17)$$

$$\frac{d\bar{W}_2}{d\bar{X}} \Big|_{\bar{X}=1} = 0, \quad \bar{W}_3 \Big|_{\bar{X}=1} = 0, \quad \frac{d\bar{W}_3}{d\bar{X}} \Big|_{\bar{X}=1} = 0. \quad (18)$$

5. CLAMPED-SIMPLY SUPPORTED

The triple-walled carbon nanotube with clamped-simply supported boundary conditions satisfy the buckling behavior's following non-dimensional boundary conditions.

$$\bar{W}_1 \Big|_{\bar{X}=0} = 0, \quad \frac{d\bar{W}_1}{d\bar{X}} \Big|_{\bar{X}=0} = 0, \quad \bar{W}_2 \Big|_{\bar{X}=0} = 0, \quad (19)$$

$$\frac{d\bar{W}_2}{d\bar{X}} \Big|_{\bar{X}=0} = 0, \quad \bar{W}_3 \Big|_{\bar{X}=0} = 0, \quad \frac{d\bar{W}_3}{d\bar{X}} \Big|_{\bar{X}=0} = 0, \quad (20)$$

$$\bar{W}_1 \Big|_{\bar{X}=1} = 0, \quad \frac{d^2\bar{W}_1}{d\bar{X}^2} \Big|_{\bar{X}=1} = 0, \quad \bar{W}_2 \Big|_{\bar{X}=1} = 0, \quad (21)$$

$$\frac{d^2\bar{W}_2}{d\bar{X}^2} \Big|_{\bar{X}=1} = 0, \quad \bar{W}_3 \Big|_{\bar{X}=1} = 0, \quad \frac{d^2\bar{W}_3}{d\bar{X}^2} \Big|_{\bar{X}=1} = 0. \quad (22)$$

6. APPROXIMATE METHODS

Since exact solutions are available for triple-walled carbon nanotube with simply-simply supported boundary conditions as $\bar{W}_1(\bar{X}) = Y_1 \sin(\pi\bar{X})$, $\bar{W}_2(\bar{X}) = Y_2 \sin(\pi\bar{X})$ [22] and $\bar{W}_3(\bar{X}) = Y_3 \sin(\pi\bar{X})$, it results in quick analytical solutions. Based on the suitable polynomial usage, the Bubnov-Galerkin method is classified here as Bubnov-Galerkin-1 (B-G-1) and Bubnov-Galerkin-2 (B-G-2). In the present analysis, two approximate methods, namely Bubnov-Galerkin and Petrov-Galerkin, estimate critical buckling loads. Since it is a triple-walled carbon nanotube, the results yield three critical buckling loads. Three different boundary conditions, namely simply-simply supported, clamped-clamped, and clamped-simply supported, are considered in the present study.

In a generic approach, the Bubnov–Galerkin Method or Petrov–Galerkin Method with weighted residual formulation using polynomial functions for any boundary conditions of triple-walled carbon nanotube takes the form as,

$$\int_0^1 \begin{vmatrix} A_{11}(\bar{X}) & A_{12}(\bar{X}) & A_{13}(\bar{X}) \\ A_{21}(\bar{X}) & A_{22}(\bar{X}) & A_{23}(\bar{X}) \\ A_{31}(\bar{X}) & A_{32}(\bar{X}) & A_{33}(\bar{X}) \end{vmatrix} \psi(\bar{X}) d\bar{X} = 0, \quad (23)$$

$$A_{11}(\bar{X}) = \frac{d^4 \bar{W}_1(\bar{X})}{d\bar{X}^4} + \beta_1 \bar{W}_1(\bar{X}) + \left(\alpha_{twn}^E \right) \frac{d^2 \bar{W}_1(\bar{X})}{d\bar{X}^2}, \quad (24)$$

$$A_{12}(\bar{X}) = -\beta_1 \bar{W}_2(\bar{X}), \quad A_{33}(\bar{X}) = 0, \quad (25)$$

$$A_{21}(\bar{X}) = -\left(\frac{\beta_1}{\delta_1} \right) \bar{W}_1(\bar{X}), \quad (26)$$

$$A_{22}(\bar{X}) = \frac{d^4 \bar{W}_2(\bar{X})}{d\bar{X}^4} + \left(\frac{\beta_1}{\delta_1} \right) \bar{W}_2(\bar{X}) + \left(\alpha_{twn}^E \right) \left(\frac{\varepsilon_1}{\delta_1} \right) \frac{d^2 \bar{W}_2(\bar{X})}{d\bar{X}^2}, \quad (27)$$

$$A_{23}(\bar{X}) = -\beta_2 \bar{W}_3(\bar{X}), \quad A_{31}(\bar{X}) = 0, \quad A_{32}(\bar{X}) = -\beta_2 \left(\frac{\delta_1}{\delta_2} \right) \bar{W}_2(\bar{X}), \quad (28)$$

$$A_{33}(\bar{X}) = \frac{d^4 \bar{W}_3(\bar{X})}{d\bar{X}^4} + \beta_2 \left(\frac{\delta_1}{\delta_2} \right) \bar{W}_3(\bar{X}) + \left(\alpha_{twn}^E \right) \left(\frac{\varepsilon_2}{\delta_2} \right) \frac{d^2 \bar{W}_3(\bar{X})}{d\bar{X}^2}. \quad (29)$$

Eq. (23) further reduces to the following form by utilising Eq. (24) to Eq. (29),

$$A_{twn} \left(\alpha_{twn}^E \right)^3 + B_{twn} \left(\alpha_{twn}^E \right)^2 + C_{twn} \left(\alpha_{twn}^E \right) + D_{twn} = 0. \quad (30)$$

Eq. (30) estimates three different values of α_{twn}^E and using Eq. (9), the Euler critical buckling loads for the innermost carbon nanotube, middle carbon nanotube, and outer nanotube are estimated.

7. SIMPLY-SIMPLY SUPPORTED AT BOTH ENDS

The present work uses the following polynomial functions for the first time by satisfying the triple-walled carbon nanotube's boundary conditions as simply-simply supported at both ends, and the Bubnov-Galerkin-1 uses the below polynomials as,

$$\bar{W}_1(\bar{X}) = D_1 \left(\frac{1}{12} \bar{X}^4 - \frac{1}{6} \bar{X}^3 + \frac{1}{12} \bar{X} \right), \quad (31)$$

$$\bar{W}_2(\bar{X}) = D_2 \left(\frac{1}{12} \bar{X}^4 - \frac{1}{6} \bar{X}^3 + \frac{1}{12} \bar{X} \right), \quad (32)$$

$$\bar{W}_3(\bar{X}) = D_3 \left(\frac{1}{12} \bar{X}^4 - \frac{1}{6} \bar{X}^3 + \frac{1}{12} \bar{X} \right), \quad (33)$$

$$\bar{\psi}_{ss}^{(4)}(\bar{X}) = \left(\frac{1}{12} \bar{X}^4 - \frac{1}{6} \bar{X}^3 + \frac{1}{12} \bar{X} \right). \quad (34)$$

It is interesting to note that the polynomials $\bar{W}_1(\bar{X}) = D_1(-3\bar{X}^5 + 10\bar{X}^3 - 7\bar{X})$, $\bar{W}_2(\bar{X}) = D_2(-3\bar{X}^5 + 10\bar{X}^3 - 7\bar{X})$, and $\bar{W}_3(\bar{X}) = D_3(-3\bar{X}^5 + 10\bar{X}^3 - 7\bar{X})$ produce the same results as previous polynomials results [Eq. (31) to Eq. (34)] using Bubnov-Galerkin-1. Also, the polynomials $\bar{W}_3 = 0$, $c_{23} = 0$, $\bar{W}_1(-\bar{X})$ and $\bar{W}_2(-\bar{X})$ yields the results of double-walled carbon nanotube proposed by Elishakoff et al [22]. For the Bubnov-Galerkin-2, polynomials take form as $\bar{W}_1(\bar{X}) = D_1(-\bar{X}^4 + 2\bar{X}^3 - \bar{X})$, $\bar{W}_2(\bar{X}) = D_2(-\bar{X}^4 + 2\bar{X}^3 - \bar{X})$, and $\bar{W}_3(\bar{X}) = D_3(-\bar{X}^4 + 2\bar{X}^3 - \bar{X})$. The Petrov-Galerkin (P-G) method evaluates the three critical buckling loads using $\bar{W}_1(\bar{X}) = D_1(-\bar{X}^4 + 2\bar{X}^3 - \bar{X})$, $\bar{W}_2(\bar{X}) = D_2(-\bar{X}^4 + 2\bar{X}^3 - \bar{X})$, and $\bar{W}_3(\bar{X}) = D_3(-\bar{X}^4 + 2\bar{X}^3 - \bar{X})$ polynomials. The weight function assumes in the form of $\bar{\psi}_{ss}^{(3)}(\bar{X}) = -\bar{X}^6 + 5\bar{X}^3 - 4\bar{X}$. If the effect of the third carbon nanotube attains as $\bar{W}_3 = 0$, $\bar{W}_1(-\bar{X})$, $\bar{W}_2(-\bar{X})$, and $c_{23} = 0$, the results estimate the critical buckling loads of double-walled carbon nanotube [22].

7.1. Explicit exact critical buckling load of simply-simply supported at both ends

Using the trigonometric functions $\bar{W}_1(\bar{X}) = Y_1 \sin(\pi\bar{X})$, $\bar{W}_2(\bar{X}) = Y_2 \sin(\pi\bar{X})$ [22] and $\bar{W}_3(\bar{X}) = Y_3 \sin(\pi\bar{X})$, the explicit expression of Exact solution is in form of Eq. (30) by following steps from Eq. (23) to Eq. (29) results,

$$A_{twn}^{Exact} = - \left(\frac{\pi^6 \epsilon_1 \epsilon_2}{8\delta_1 \delta_2} \right), \quad (35)$$

$$B_{twn}^{Exact} = \left(\frac{\pi^8 \epsilon_1}{8\delta_1} \right) + \left(\frac{[\pi^4 \beta_2 (\epsilon_1 + \epsilon_2)]}{8\delta_2} \right) + \left(\frac{\pi^8 \epsilon_2}{8\delta_2} \right) + \left(\frac{[\pi^4 \beta_1 \epsilon_2 (1 + \epsilon_1)]}{8\delta_1 \delta_2} \right) + \left(\frac{\pi^8 \epsilon_1 \epsilon_2}{8\delta_1 \delta_2} \right), \quad (36)$$

$$C_{twn}^{Exact} = - \left(\frac{\pi^{10} \epsilon_2}{8\delta_2} \right) - \left(\frac{[\pi^6 \beta_1 \epsilon_2] + (\pi^6 \beta_2 [\epsilon_1 + \epsilon_2 + \delta_1])}{8\delta_2} \right) - \left(\frac{[\pi^2 \beta_1 \beta_2 (1 + \epsilon_1 + \epsilon_2)]}{8\delta_2} \right) - \frac{\pi^6 \beta_1 \epsilon_2}{8\delta_1 \delta_2} - \left(\frac{\pi^{10} \epsilon_1}{8\delta_1} \right) - \left(\frac{[\pi^6 \beta_1 (1 + \epsilon_1)]}{8\delta_1} \right) - \left(\frac{\pi^{10}}{8} \right) - \left(\frac{\pi^6 \beta_2}{8} \right), \quad (37)$$

$$D_{twn}^{Exact} = \left(\frac{\pi^8 \beta_1}{8\delta_1} \right) + \left(\frac{\pi^8 \beta_2 \delta_1}{8\delta_2} \right) + \left(\frac{[\pi^4 \beta_1 \beta_2 (1 + \delta_1)]}{8\delta_2} \right) + \left(\frac{\pi^{12}}{8} \right) + \left(\frac{[\pi^8 (\beta_1 + \beta_2)]}{8} \right) + \left(\frac{\pi^4 \beta_1 \beta_2}{8} \right). \quad (38)$$

The three different values of α_{twn}^E from Eq. (30) compute the innermost, middle, and outer nanotube's exact Euler critical buckling load for the triple-walled carbon nanotube using Eq. (9).

7.2. Explicit critical buckling load based on Bubnov-Galerkin-1 method of simply simply supported at both ends

With the help of Eq. (31) to Eq. (34) for Bubnov-Galerkin-1 method, as mentioned earlier, Euler critical buckling loads for innermost, middle, and outer nanotubes result from solving Eq. (30) using Eq. (9). The relevant coefficients of Eq. (30) is in the form of,

$$A_{twn}^{BG-1} = - \left(\frac{4913\epsilon_1\epsilon_2}{128024064000\delta_1\delta_2} \right), \quad (39)$$

$$B_{twn}^{BG-1} = \left(\frac{289\epsilon_1}{762048000\delta_1} \right) + \left(\frac{[8959\beta_2(\epsilon_1 + \epsilon_2)]}{2304433152000\delta_2} \right) + \left(\frac{289\epsilon_2}{762048000\delta_2} \right) \\ + \left(\frac{[8959\beta_1\epsilon_2(1 + \epsilon_1)]}{2304433152000\delta_1\delta_2} \right) + \left(\frac{289\epsilon_1\epsilon_2}{762048000\delta_1\delta_2} \right), \quad (40)$$

$$C_{twn}^{BG-1} = - \left(\frac{17\epsilon_2}{4536000\delta_2} \right) - \left(\frac{[527\beta_1\epsilon_2] + (527\beta_2[\epsilon_1 + \epsilon_2 + \delta_1])}{13716864000\delta_2} \right) \\ - \left(\frac{[16337\beta_1\beta_2(1 + \epsilon_1 + \epsilon_2)]}{41479796736000\delta_2} \right) - \frac{527\beta_1\epsilon_2}{13716864000\delta_1\delta_2} \quad (41) \\ - \left(\frac{17\epsilon_1}{4536000\delta_1} \right) - \left(\frac{[527\beta_1(1 + \epsilon_1)]}{13716864000\delta_1} \right) - \left(\frac{17}{4536000} \right) - \left(\frac{527\beta_2}{13716864000} \right),$$

$$D_{twn}^{BG-1} = \left(\frac{31\beta_1}{81648000\delta_1} \right) + \left(\frac{31\beta_2\delta_1}{81648000\delta_2} \right) + \left(\frac{[961\beta_1\beta_2(1 + \delta_1)]}{246903552000\delta_2} \right) + \left(\frac{1}{27000} \right) \\ + \left(\frac{[31(\beta_1 + \beta_2)]}{81648000} \right) + \left(\frac{961\beta_1\beta_2}{246903552000} \right). \quad (42)$$

7.3. Explicit critical buckling load based on Bubnov-Galerkin-2 method of simply simply supported at both ends

The Bubnov-Galerkin-2 method with appropriate polynomials discussed earlier results in the following explicit expression, and it is in the form of Eq. (30),

$$A_{twn}^{BG-2} = - \left(\frac{4913\epsilon_1\epsilon_2}{42875\delta_1\delta_2} \right), \quad (43)$$

$$B_{twn}^{BG-2} = \left(\frac{6936\epsilon_1}{6125\delta_1} \right) + \left(\frac{[8959\beta_2(\epsilon_1 + \epsilon_2)]}{771750\delta_2} \right) + \left(\frac{6936\epsilon_2}{6125\delta_2} \right) \\ + \left(\frac{[8959\beta_1\epsilon_2(1 + \epsilon_1)]}{771750\delta_1\delta_2} \right) + \left(\frac{6936\epsilon_1\epsilon_2}{6125\delta_1\delta_2} \right), \quad (44)$$

$$C_{twn}^{BG-2} = - \left(\frac{9792\epsilon_2}{875\delta_2} \right) - \left(\frac{[2108\beta_1\epsilon_2] + (2108\beta_2[\epsilon_1 + \epsilon_2 + \delta_1])}{18375\delta_2} \right) \\ - \left(\frac{[16337\beta_1\beta_2(1 + \epsilon_1 + \epsilon_2)]}{13891500\delta_2} \right) - \frac{2108\beta_1\epsilon_2}{18375\delta_1\delta_2} - \left(\frac{9792\epsilon_1}{875\delta_1} \right) \quad (45) \\ - \left(\frac{[2108\beta_1(1 + \epsilon_1)]}{18375\delta_1} \right) - \left(\frac{9792}{875} \right) - \left(\frac{2108\beta_2}{18375} \right),$$

$$D_{twn}^{BG-2} = \left(\frac{992\beta_1}{875\delta_1} \right) + \left(\frac{992\beta_2\delta_1}{875\delta_2} \right) + \left(\frac{[1922\beta_1\beta_2(1+\delta_1)]}{165375\delta_2} \right) + \left(\frac{13824}{125} \right) \\ + \left(\frac{[992(\beta_1 + \beta_2)]}{875} \right) + \left(\frac{1922\beta_1\beta_2}{165375} \right). \quad (46)$$

Eq. (9) helps in the determination of Euler's critical buckling load of Bubnov-Galerkin-2 by solving Eq. (30) for innermost, middle and outer nanotube using the above Eq. (43) to Eq. (46).

7.4. Explicit critical buckling load based on Petrov-Galerkin-1 method of simply-simply supported at both ends

The solution of Eq. (30) derived from the Petrov-Galerkin-1 method by utilizing the relevant polynomials as discussed previously yields the three different Euler critical buckling loads of triple-walled nanotube with the help of Eq. (9). The explicit expression is in the form of,

$$A_{twn}^{PG-1} = - \left(\frac{2197\epsilon_1\epsilon_2}{216\delta_1\delta_2} \right), \quad (47)$$

$$B_{twn}^{PG-1} = \left(\frac{4225\epsilon_1}{42\delta_1} \right) + \left(\frac{[28561\beta_2(\epsilon_1 + \epsilon_2)]}{27720\delta_2} \right) \\ + \left(\frac{4225\epsilon_2}{42\delta_2} \right) + \left(\frac{[28561\beta_1\epsilon_2(1 + \epsilon_1)]}{27720\delta_1\delta_2} \right) + \left(\frac{4225\epsilon_1\epsilon_2}{42\delta_1\delta_2} \right), \quad (48)$$

$$C_{twn}^{PG-1} = - \left(\frac{48750\epsilon_2}{49\delta_2} \right) - \left(\frac{[10985\beta_1\epsilon_2] + [10985\beta_2(\epsilon_1 + \epsilon_2 + \delta_1)]}{1078\delta_2} \right) \\ - \left(\frac{[371293\beta_1\beta_2(1 + \epsilon_1 + \epsilon_2)]}{3557400\delta_2} \right) - \frac{10985\beta_1\epsilon_2}{1078\delta_1\delta_2} - \left(\frac{48750\epsilon_1}{49\delta_1} \right) \\ - \left(\frac{[10985\beta_1(1 + \epsilon_1)]}{1078\delta_1} \right) - \left(\frac{48750}{49} \right) - \left(\frac{10985\beta_2}{1078} \right), \quad (49)$$

$$D_{twn}^{PG-1} = \left(\frac{380250\beta_1}{3773\delta_1} \right) + \left(\frac{380250\beta_2\delta_1}{3773\delta_2} \right) + \left(\frac{[85683\beta_1\beta_2(1 + \delta_1)]}{83006\delta_2} \right) \\ + \left(\frac{3375000}{343} \right) + \left(\frac{[380250(\beta_1 + \beta_2)]}{3773} \right) + \left(\frac{85683\beta_1\beta_2}{83006} \right). \quad (50)$$

8. CLAMPED AT BOTH ENDS

Since the exact solution is not available for clamped-clamped boundary conditions, the Bubnov-Galerkin-1, Bubnov-Galerkin-2, and Petrov-Galerkin methods evaluate the critical buckling loads based on different polynomials for triple-walled carbon nanotube. The Bubnov-Galerkin-1 method computes the critical buckling loads of triple-walled carbon nanotube for clamped-clamped boundary conditions using the Filonenko-Borodich trigonometric polynomials $\bar{W}_1(\bar{X}) = Y_1 [1 - \cos(2\pi\bar{X})]$, $\bar{W}_2(\bar{X}) = Y_2 [1 - \cos(2\pi\bar{X})]$ [22], and $\bar{W}_3(\bar{X}) = Y_3 [1 - \cos(2\pi\bar{X})]$. Using the polynomials as

$$\bar{W}_1(\bar{X}) = D_1 \left(\frac{1}{12} \bar{X}^4 - \frac{1}{6} \bar{X}^3 + \frac{1}{12} \bar{X}^2 \right), \quad (51)$$

$$\bar{W}_2(\bar{X}) = D_2 \left(\frac{1}{12} \bar{X}^4 - \frac{1}{6} \bar{X}^3 + \frac{1}{12} \bar{X}^2 \right), \quad (52)$$

$$\bar{W}_3(\bar{X}) = D_3 \left(\frac{1}{12} \bar{X}^4 - \frac{1}{6} \bar{X}^3 + \frac{1}{12} \bar{X}^2 \right), \quad (53)$$

$$\bar{\psi}_{cc}^{(4)}(\bar{X}) = \left(\frac{1}{12} \bar{X}^4 - \frac{1}{6} \bar{X}^3 + \frac{1}{12} \bar{X}^2 \right), \quad (54)$$

the Bubnov-Galerkin-2 method estimates the critical buckling loads for the triple-walled carbon nanotube. It is interesting to observe that the polynomials $\bar{W}_1(\bar{X}) = D_1(-\bar{X}^4 + 2\bar{X}^3 - \bar{X}^2)$, $\bar{W}_2(\bar{X}) = D_2(-\bar{X}^4 + 2\bar{X}^3 - \bar{X}^2)$, and $\bar{W}_3(\bar{X}) = D_3(-\bar{X}^4 + 2\bar{X}^3 - \bar{X}^2)$, used in the Bubnov-Galerkin-2 estimates the same results as compared with earlier polynomials [Eq. (51) to Eq. (54)]. In evaluating critical buckling loads for triple-walled carbon nanotubes using the Petrov-Galerkin method, the polynomials assume in the form of $\bar{W}_1(\bar{X}) = D_1(-\bar{X}^4 + 2\bar{X}^3 - \bar{X}^2)$, $\bar{W}_2(\bar{X}) = D_2(-\bar{X}^4 + 2\bar{X}^3 - \bar{X}^2)$, and $\bar{W}_3(\bar{X}) = D_3(-\bar{X}^4 + 2\bar{X}^3 - \bar{X}^2)$. The weight function takes the form of $\bar{\psi}_{cc}^{(2)}(\bar{X}) = 1 - \cos(2\pi\bar{X})$ [22]. In the value of $\bar{W}_3 = 0$, $\bar{W}_1(-\bar{X})$, $\bar{W}_2(-\bar{X})$, and $c_{23} = 0$, the critical buckling load yields the results of a double-walled carbon nanotube [22].

8.1. Explicit critical buckling load based on Bubnov-Galerkin-1 method of clamped at both ends

Using the Filonenko-Borodich trigonometric polynomials discussed earlier, the Bubnov-Galerkin-1 method results in the following explicit form by utilizing the steps Eq. (24) to Eq. (30),

$$A_{twn}^{BG-1} = - \left(\frac{8\pi^6 \epsilon_1 \epsilon_2}{\delta_1 \delta_2} \right), \quad (55)$$

$$B_{twn}^{BG-1} = \left(\frac{32\pi^8 \epsilon_1}{\delta_1} \right) + \left(\frac{[6\pi^4 \beta_2 (\epsilon_1 + \epsilon_2)]}{\delta_2} \right) + \left(\frac{32\pi^8 \epsilon_2}{\delta_2} \right) \\ + \left(\frac{[6\pi^4 \beta_1 \epsilon_2 (1 + \epsilon_1)]}{\delta_1 \delta_2} \right) + \left(\frac{32\pi^8 \epsilon_1 \epsilon_2}{\delta_1 \delta_2} \right), \quad (56)$$

$$C_{twn}^{BG-1} = - \left(\frac{128\pi^{10} \epsilon_2}{\delta_2} \right) - \left(\frac{[24\pi^6 \beta_1 \epsilon_2] + (24\pi^6 \beta_2 [\epsilon_1 + \epsilon_2 + \delta_1])}{\delta_2} \right) \\ - \left(\frac{[9\pi^2 \beta_1 \beta_2 (1 + \epsilon_1 + \epsilon_2)]}{\delta_2} \right) - \frac{24\pi^6 \beta_1 \epsilon_2}{\delta_1 \delta_2} - \left(\frac{128\pi^{10} \epsilon_1}{\delta_1} \right) \\ - \left(\frac{[24\pi^6 \beta_1 (1 + \epsilon_1)]}{\delta_1} \right) - \left(\frac{128\pi^{10}}{1} \right) - \left(\frac{24\pi^6 \beta_2}{1} \right), \quad (57)$$

$$D_{twn}^{BG-1} = \left(\frac{96\pi^8 \beta_1}{\delta_1} \right) + \left(\frac{96\pi^8 \beta_2 \delta_1}{\delta_2} \right) + \left(\frac{[18\pi^4 \beta_1 \beta_2 (1 + \delta_1)]}{\delta_2} \right) + \left(\frac{512\pi^{12}}{1} \right) \\ + \left(\frac{[96\pi^8 (\beta_1 + \beta_2)]}{1} \right) + \left(\frac{18\pi^4 \beta_1 \beta_2}{1} \right). \quad (58)$$

The three different Euler's critical buckling loads for Bubnov-Galerkin-1 results are estimated by substituting the above expressions in Eq. (30) and Eq. (9).

8.2. Explicit critical buckling load based on Bubnov-Galerkin-2 method of clamped at both ends

The explicit expression of Eq. (30) arranges in the following form with the usage of Eq. (51) to Eq. (54) by adhering the procedures from Eq. (23) to Eq. (29).

$$A_{twn}^{BG-2} = - \left(\frac{432081216000 \epsilon_1 \epsilon_2}{\delta_1 \delta_2} \right), \quad (59)$$

$$B_{twn}^{BG-2} = \left(\frac{\epsilon_1}{10287648000 \delta_1} \right) + \left(\frac{[\beta_2 (\epsilon_1 + \epsilon_2)]}{5184974592000 \delta_2} \right) + \left(\frac{\epsilon_2}{10287648000 \delta_2} \right) \\ + \left(\frac{[\beta_1 \epsilon_2 (1 + \epsilon_1)]}{5184974592000 \delta_1 \delta_2} \right) + \left(\frac{\epsilon_1 \epsilon_2}{10287648000 \delta_1 \delta_2} \right), \quad (60)$$

$$C_{twn}^{BG-2} = - \left(\frac{\epsilon_2}{244944000 \delta_2} \right) - \left(\frac{[\beta_1 \epsilon_2] + (\beta_2 [\epsilon_1 + \epsilon_2 + \delta_1])}{123451776000 \delta_2} \right) \\ - \left(\frac{[\beta_1 \beta_2 (1 + \epsilon_1 + \epsilon_2)]}{62219695104000 \delta_2} \right) - \frac{\beta_1 \epsilon_2}{123451776000 \delta_1 \delta_2} - \left(\frac{\epsilon_1}{244944000 \delta_1} \right) \\ - \left(\frac{[\beta_1 (1 + \epsilon_1)]}{123451776000 \delta_1} \right) - \left(\frac{1}{244944000} \right) - \left(\frac{\beta_2}{123451776000} \right), \quad (61)$$

$$D_{twn}^{BG-2} = \left(\frac{\beta_1}{2939328000 \delta_1} \right) + \left(\frac{\beta_2 \delta_1}{2939328000 \delta_2} \right) + \left(\frac{[\beta_1 \beta_2 (1 + \delta_1)]}{1481421312000 \delta_2} \right) \\ + \left(\frac{1}{5832000} \right) + \left(\frac{[(\beta_1 + \beta_2)]}{2939328000} \right) + \left(\frac{\beta_1 \beta_2}{1481421312000} \right). \quad (62)$$

From the above coefficients, the evaluation of Euler's critical buckling loads of innermost, middle, and outer nanotube happens with the help of Eq. (30) and Eq. (9).

8.3. Explicit critical buckling load based on Petrov-Galerkin-1 method of clamped at both ends

The determination of the innermost, middle, and outer nanotube's Euler critical buckling loads is computed from the Petrov-Galerkin-1 method with the help of the appropriate polynomials discussed previously. The explicit expression for the coefficients is in the form of Eq. (30) as follows,

$$A_{twn}^{PG-1} = + \frac{216 \epsilon_1 \epsilon_2}{\pi^6 \delta_1 \delta_2}, \quad (63)$$

$$B_{twn}^{PG-1} = - \left(\frac{864\epsilon_1}{\pi^4\delta_1} \right) + \left(-\frac{54\beta_2\epsilon_1}{\pi^8\delta_2} - \frac{6\beta_2\epsilon_1}{5\pi^4\delta_2} - \frac{54\beta_2\epsilon_2}{\pi^8\delta_2} - \frac{6\beta_2\epsilon_2}{5\pi^4\delta_2} \right) - \left(\frac{864\epsilon_2}{\pi^4\delta_2} \right) \quad (64)$$

$$+ \left(-\frac{54\beta_1\epsilon_2}{\pi^8\delta_1\delta_2} - \frac{6\beta_1\epsilon_2}{5\pi^4\delta_1\delta_2} - \frac{54\beta_1\epsilon_1\epsilon_2}{\pi^8\delta_1\delta_2} - \frac{6\beta_1\epsilon_1\epsilon_2}{5\pi^4\delta_1\delta_2} \right) - \left(\frac{864\epsilon_1\epsilon_2}{\pi^4\delta_1\delta_2} \right),$$

$$C_{twn}^{PG-1} = + \left(\frac{3456\epsilon_2}{\pi^2\delta_2} \right) + \left(\frac{216\beta_1\epsilon_2}{\pi^6\delta_2} + \frac{24\beta_1\epsilon_2}{5\pi^2\delta_2} + \frac{24\beta_2\epsilon_1}{5\pi^2\delta_2} + \frac{216\beta_2\epsilon_1}{\pi^6\delta_2} + \frac{24\beta_2\epsilon_2}{5\pi^2\delta_2} \right)$$

$$+ \left(\frac{216\beta_2\epsilon_2}{\pi^6\delta_2} + \frac{24\beta_2\delta_1}{5\pi^2\delta_2} + \frac{216\beta_2\delta_1}{\pi^6\delta_2} \right) + \left(\frac{27\beta_1\beta_2}{2\pi^{10}\delta_2} + \frac{\beta_1\beta_2}{150\pi^2\delta_2} + \frac{3\beta_1\beta_2}{5\pi^6\delta_2} + \frac{27\beta_1\beta_2\epsilon_1}{2\pi^{10}\delta_2} \right)$$

$$+ \left(\frac{\beta_1\beta_2\epsilon_1}{150\pi^2\delta_2} + \frac{3\beta_1\beta_2\epsilon_1}{5\pi^6\delta_2} + \frac{27\beta_1\beta_2\epsilon_2}{2\pi^{10}\delta_2} + \frac{\beta_1\beta_2\epsilon_2}{150\pi^2\delta_2} + \frac{3\beta_1\beta_2\epsilon_2}{5\pi^6\delta_2} \right)$$

$$+ \left(\frac{216\beta_1\epsilon_2}{\pi^6\delta_1\delta_2} + \frac{24\beta_1\epsilon_2}{5\pi^2\delta_1\delta_2} \right) + \left(\frac{3456\epsilon_1}{\pi^2\delta_1} \right) + \left(\frac{216\beta_1}{\pi^6\delta_1} + \frac{24\beta_1}{5\pi^2\delta_1} + \frac{216\beta_1\epsilon_1}{\pi^6\delta_1} + \frac{24\beta_1\epsilon_1}{5\pi^2\delta_1} \right)$$

$$+ \left(\frac{3456}{\pi^2} \right) + \left(\frac{24\beta_2}{5\pi^2} + \frac{216\beta_2}{\pi^6} \right), \quad (65)$$

$$D_{twn}^{PG-1} = \left(-\frac{96\beta_1}{5\delta_1} - \frac{864\beta_1}{\pi^4\delta_1} \right) + \left(-\frac{96\beta_2\delta_1}{5\delta_2} - \frac{864\beta_2\delta_1}{\pi^4\delta_2} \right) + \left(-\frac{2\beta_1\beta_2}{75\delta_2} - \frac{12\beta_1\beta_2}{5\pi^4\delta_2} \right)$$

$$+ \left(-\frac{54\beta_1\beta_2}{\pi^8\delta_2} - \frac{2\beta_1\beta_2\delta_1}{75\delta_2} - \frac{12\beta_1\beta_2\delta_1}{5\pi^4\delta_2} - \frac{54\beta_1\beta_2\delta_1}{\pi^8\delta_2} \right) + (-13824)$$

$$+ \left(-\frac{96\beta_1}{5} - \frac{864\beta_1}{\pi^4} \right) + \left(-\frac{96\beta_2}{5} - \frac{864\beta_2}{\pi^4} \right) + \left(-\frac{2\beta_1\beta_2}{75} - \frac{12\beta_1\beta_2}{5\pi^4} - \frac{54\beta_1\beta_2}{\pi^8} \right). \quad (66)$$

Further, the three different Euler's critical loads for innermost, middle, and outer nanotube are computed using the above expression using Eq. (30) and Eq. (9).

9. CLAMPED-SIMPLY SUPPORTED

The Bubnov-Galerkin-1 method uses the polynomials as

$$\bar{W}_1(\bar{X}) = D_1 \left(\frac{1}{12}\bar{X}^4 - \frac{5}{24}\bar{X}^3 + \frac{1}{8}\bar{X}^2 \right), \quad (67)$$

$$\bar{W}_2(\bar{X}) = D_2 \left(\frac{1}{12}\bar{X}^4 - \frac{5}{24}\bar{X}^3 + \frac{1}{8}\bar{X}^2 \right), \quad (68)$$

$$\bar{W}_3(\bar{X}) = D_3 \left(\frac{1}{12}\bar{X}^4 - \frac{5}{24}\bar{X}^3 + \frac{1}{8}\bar{X}^2 \right), \quad (69)$$

$$\bar{\psi}_{cs}^{(4)}(\bar{X}) = \left(\frac{1}{12}\bar{X}^4 - \frac{5}{24}\bar{X}^3 + \frac{1}{8}\bar{X}^2 \right), \quad (70)$$

for the clamped-simply supported boundary conditions to evaluate the critical buckling loads of triple-walled carbon nanotube. Incidentally, the following polynomials

$\bar{W}_1(\bar{X}) = D_1(-2\bar{X}^4 + 3\bar{X}^3 - \bar{X})$, $\bar{W}_2(\bar{X}) = D_2(-2\bar{X}^4 + 3\bar{X}^3 - \bar{X})$, and $\bar{W}_3(\bar{X}) = D_3(-2\bar{X}^4 + 3\bar{X}^3 - \bar{X})$ satisfy the triple-walled carbon nanotube with clamped-simply supported boundary condition computes the same critical buckling load results estimated by Eq. (67) to Eq. (70). With the help of three polynomials as $\bar{W}_1(\bar{X}) = D_1(5X^5 - 16X^4 + 14X^3 - 3X)$, $\bar{W}_2(\bar{X}) = D_2(5X^5 - 16X^4 + 14X^3 - 3X)$, and $\bar{W}_3(\bar{X}) = D_3(5X^5 - 16X^4 + 14X^3 - 3X)$, the Bubnov-Galerkin-2 method helps to estimate the three critical buckling loads. The Petrov-Galerkin method computes the critical buckling loads of triple-walled carbon nanotube utilizing the three polynomials as $\bar{W}_1(\bar{X}) = D_1(-2\bar{X}^4 + 3\bar{X}^3 - \bar{X})$, $\bar{W}_2(\bar{X}) = D_2(-2\bar{X}^4 + 3\bar{X}^3 - \bar{X})$, and $\bar{W}_3(\bar{X}) = D_3(-2\bar{X}^4 + 3\bar{X}^3 - \bar{X})$. Also, the weight function considers in the form of $\psi_{cs}^{(3)}(\bar{X}) = (5X^5 - 16X^4 + 14X^3 - 3X)$. If the polynomials reach the value of $\bar{W}_3 = 0$, $\bar{W}_1(-\bar{X})$, $\bar{W}_2(-\bar{X})$, and $c_{23} = 0$ yield the results of double-walled carbon nanotube's critical buckling load results [22].

9.1. Explicit critical buckling load based on Bubnov-Galerkin-1 method of clamped-simply supported

By following the steps from Eq. (23) to Eq. (29) with the substitution of Eq. (67) to Eq. (70) appropriately, the explicit expression takes the form of (30) and the coefficients are,

$$A_{twn}^{BG-1} = - \left(\frac{\epsilon_1 \epsilon_2}{4741632000 \delta_1 \delta_2} \right), \quad (71)$$

$$B_{twn}^{BG-1} = \left(\frac{\epsilon_1}{225792000 \delta_1} \right) + \left(\frac{[19\beta_2(\epsilon_1 + \epsilon_2)]}{1024192512000 \delta_2} \right) + \left(\frac{\epsilon_2}{225792000 \delta_2} \right) \\ + \left(\frac{[19\beta_1\epsilon_2(1 + \epsilon_1)]}{1024192512000 \delta_1 \delta_2} \right) + \left(\frac{\epsilon_1 \epsilon_2}{225792000 \delta_1 \delta_2} \right), \quad (72)$$

$$C_{twn}^{BG-1} = - \left(\frac{\epsilon_2}{10752000 \delta_2} \right) - \left(\frac{[19\beta_1\epsilon_2] + (19\beta_2[\epsilon_1 + \epsilon_2 + \delta_1])}{48771072000 \delta_2} \right) \\ - \left(\frac{[361\beta_1\beta_2(1 + \epsilon_1 + \epsilon_2)]}{221225582592000 \delta_2} \right) - \frac{19\beta_1\epsilon_2}{48771072000 \delta_1 \delta_2} - \left(\frac{\epsilon_1}{10752000 \delta_1} \right) \\ - \left(\frac{[19\beta_1(1 + \epsilon_1)]}{48771072000 \delta_1} \right) - \left(\frac{1}{10752000} \right) - \left(\frac{19\beta_2}{48771072000} \right), \quad (73)$$

$$D_{twn}^{BG-1} = \left(\frac{19\beta_1}{2322432000 \delta_1} \right) + \left(\frac{\beta_2 \delta_1}{2322432000 \delta_2} \right) + \left(\frac{[361\beta_1\beta_2(1 + \delta_1)]}{10534551552000 \delta_2} \right) \\ + \left(\frac{1}{512000} \right) + \left(\frac{[19(\beta_1 + \beta_2)]}{2322432000} \right) + \left(\frac{\beta_1 \beta_2}{10534551552000} \right). \quad (74)$$

The above expression is evaluated for the three different Euler's critical buckling for innermost, middle, and outer nanotubes, respectively, using Eq. (30) and Eq. (9).

9.2. Explicit critical buckling load based on Bubnov Galerkin-2 method of clamped-simply supported

For the explicit expression of the Bubnov-Galerkin-2 method with relevant polynomials discussed earlier, the coefficients come in the form of the following methodology adopted from Eq. (23) to Eq. (29),

$$A_{twn}^{BG-2} = - \left(\frac{425259008\epsilon_1\epsilon_2}{31255875\delta_1\delta_2} \right), \quad (75)$$

$$B_{twn}^{BG-2} = \left(\frac{36192256\epsilon_1}{128625\delta_1} \right) + \left(\frac{[4524032\beta_2(\epsilon_1 + \epsilon_2)]}{4244625\delta_2} \right) + \left(\frac{36192256\epsilon_2}{128625\delta_2} \right) \\ + \left(\frac{[4524032\beta_1\epsilon_2(1 + \epsilon_1)]}{4244625\delta_1\delta_2} \right) + \left(\frac{36192256\epsilon_1\epsilon_2}{128625\delta_1\delta_2} \right), \quad (76)$$

$$C_{twn}^{BG-2} = - \left(\frac{249495552\epsilon_2}{42875\delta_2} \right) - \left(\frac{[10395648\beta_1\epsilon_2] + (10395648\beta_2[\epsilon_1 + \epsilon_2 + \delta_1])}{471625\delta_2} \right) \\ - \left(\frac{[433152\beta_1\beta_2(1 + \epsilon_1 + \epsilon_2)]}{5187875\delta_2} \right) - \frac{10395648\beta_1\epsilon_2}{471625\delta_1\delta_2} - \left(\frac{249495552\epsilon_1}{42875\delta_1} \right) \\ - \left(\frac{[10395648\beta_1(1 + \epsilon_1)]}{471625\delta_1} \right) - \left(\frac{249495552}{42875} \right) - \left(\frac{10395648\beta_2}{471625} \right), \quad (77)$$

$$D_{twn}^{BG-2} = \left(\frac{214990848\beta_1}{471625\delta_1} \right) + \left(\frac{214990848\beta_2\delta_1}{471625\delta_2} \right) + \left(\frac{[8957952\beta_1\beta_2(1 + \delta_1)]}{5187875\delta_2} \right) \\ + \left(\frac{5159780352}{42875} \right) + \left(\frac{[214990848(\beta_1 + \beta_2)]}{471625} \right) + \left(\frac{8957952\beta_1\beta_2}{5187875} \right). \quad (78)$$

The Euler's critical buckling loads for innermost, middle, and outer nanotube for Bubnov-Galerkin-2 methods are computed using the above expression with the help of Eq. (30) and Eq. (9).

9.3. Explicit critical buckling load based on Petrov-Galerkin-1 method of clamped-simply supported

The Petrov-Galerkin-1 Method with appropriate polynomials discussed previously by computing the Eq. (23) to Eq. (30), the explicit expression is in the following form,

$$A_{twn}^{PG-1} = - \left(\frac{29791\epsilon_1\epsilon_2}{42875\delta_1\delta_2} \right), \quad (79)$$

$$B_{twn}^{PG-1} = \left(\frac{84568\epsilon_1}{6125\delta_1} \right) + \left(\frac{[45167\beta_2(\epsilon_1 + \epsilon_2)]}{771750\delta_2} \right) + \left(\frac{84568\epsilon_2}{6125\delta_2} \right) \\ + \left(\frac{[45167\beta_1\epsilon_2(1 + \epsilon_1)]}{771750\delta_1\delta_2} \right) + \left(\frac{84568\epsilon_1\epsilon_2}{6125\delta_1\delta_2} \right), \quad (80)$$

$$\begin{aligned}
C_{twn}^{PG-1} = & - \left(\frac{240064\epsilon_2}{875\delta_2} \right) - \left(\frac{[64108\beta_1\epsilon_2] + (64108\beta_2 [\epsilon_1 + \epsilon_2 + \delta_1])}{55125\delta_2} \right) \\
& - \left(\frac{[68479\beta_1\beta_2 (1 + \epsilon_1 + \epsilon_2)]}{13891500\delta_2} \right) - \frac{64108\beta_1\epsilon_2}{55125\delta_1\delta_2} - \left(\frac{240064\epsilon_1}{875\delta_1} \right) \\
& - \left(\frac{[64108\beta_1 (1 + \epsilon_1)]}{55125\delta_1} \right) - \left(\frac{240064}{875} \right) - \left(\frac{64108\beta_2}{55125} \right), \tag{81}
\end{aligned}$$

$$\begin{aligned}
D_{twn}^{PG-1} = & \left(\frac{181984\beta_1}{7875\delta_1} \right) + \left(\frac{181984\beta_2\delta_1}{7875\delta_2} \right) + \left(\frac{[48598\beta_1\beta_2 (1 + \delta_1)]}{496125\delta_2} \right) + \left(\frac{681472}{125} \right) \\
& + \left(\frac{[181984 (\beta_1 + \beta_2)]}{7875} \right) + \left(\frac{48598\beta_1\beta_2}{496125} \right). \tag{82}
\end{aligned}$$

So the coefficients of the above expressions are solved to estimate the Euler's critical buckling loads of nanotube for innermost, middle, and outer nanotube with the help of Eq. (30) and Eq. (9).

10. DISCUSSIONS

The classification of nanotubes takes place like short nanotubes ($L/D < 10$) [24] or sufficiently long nanotubes ($10 < L/D < 50$) [24] or more. The outer diameter of a multi-walled carbon nanotube ranges from 2 nm to 100 nm [25]. Also, the length of multi-walled carbon nanotube varies from 0.2 μm to several μm [25] with experimental observation. It corresponds to the L/D ranges from 100, 250, 1000, or higher for the multi-walled carbon nanotubes. So the present continuum model analysis considers the triple-walled carbon nanotube as a straight nanotube structure, although its length-outer diameter ratio can be high. But, the nanotube is in a curve shape when it is long (like hair). Based on the chiral indices (n, m) [26], the carbon nanotube is in the form of the armchair (n, n) , or zigzag $(n, 0)$, or chiral nanotube $(n \neq m)$. For the single-walled carbon nanotube, the diameter in terms of the chiral vector is defined by

$D_{swcn} = \sqrt{3}a_{C-C} \frac{\sqrt{n^2 + nm + m^2}}{\pi}$ [27]. For the triple-walled carbon nanotube, the chiral indices take from as $(n, m)(n, m)(n, m)$. In particular, the chirality of triple-walled nanotube $(15, 16)$, $(14, 17)$, and $(13, 18)$ yields the diameter $D_{twn} = 14 \text{ \AA}$. Similarly, the diameter of $D_{twn} = 21 \text{ \AA}$ with chirality $(15, 16)$, $(14, 17)$ and $(13, 18)$ is arrived. So the different diameter of the nanotube estimates many chiral possibilities of triple-walled carbon nanotubes. But the continuum model used in the present buckling analysis doesn't consider the nanotube's chirality effect.

The van der Waals interaction coefficient [28] of the nanotube is defined by, $c_{(N)(N+1)} = \frac{320 \times (2R_N) \text{ erg/cm}^2}{0.16a_{C-C}^2}$, $a_{C-C} = 0.142 \text{ nm}$, $N = 1, 2$. The first and second adjacent concentric nanotubes using the distributed springs all along the circumference [28] are modeled by van der Waals interaction coefficient c_{12} . Similarly, the second and third adjacent nanotube [28] experiences the effect of van der Waals interaction coefficient c_{23} . The

present analysis calculates the moment of inertia and cross-sectional areas using the wall thickness of the nanotube suggested by Sears and Batra [29]. The moment of inertia [29] of the three nanotubes such as I_1 , I_2 , and I_3 is estimated using the expression in terms of the wall thickness of the nanotube t_h as, $I_i(t_h) = \frac{\pi}{4} \left[\left(R_i + \frac{t_h}{2} \right)^4 - \left(R_i - \frac{t_h}{2} \right)^4 \right]$, $i = 1, 2, 3$. Similarly, the cross-sectional areas [29] of nanotubes A_1 , A_2 , and A_3 are determined by $A_i(t_h) = \pi \left[\left(R_i + \frac{t_h}{2} \right)^2 - \left(R_i - \frac{t_h}{2} \right)^2 \right]$, $i = 1, 2, 3$. The mechanical properties of the triple-walled nanotube are $E = 1.0$ TPa, $R_1 = 0.35$ nm, $R_2 = 0.70$ nm, $R_3 = 1.05$ nm, $D_o = 2.10$ nm, $t_h = 0.34$ nm, $\varepsilon_2/\varepsilon_1 = 1.5$, $\delta_2/\delta_1 = 3.27057$, $\beta_2/\beta_1 = 0.291771$, $c_{12} = 69.43$ GPa and $c_{23} = 138.86$ GPa [16]. In the present investigation, the Bubnov–Galerkin and Petrov–Galerkin methods estimate the Euler’s critical buckling of triple-walled carbon nanotube. For the triple-walled carbon nanotubes with simply-simply supported boundary conditions, the accurate estimation of the Euler critical buckling is possible using exact solutions. The Bubnov–Galerkin Method is named Bubnov-Galerkin-1 and Bubnov-Galerkin-2 based on different polynomials in the present analysis. In addition to these methods, the Petrov–Galerkin method determines the critical buckling load. Developing the analytical solutions for triple-walled nanotube supported with the clamped-clamped and clamped-hinged is cumbersome. So to obtain a quick and reasonably reliable estimation, the Bubnov–Galerkin and Petrov–Galerkin method determine the critical buckling load. All the polynomials [22] used in these methods satisfy the respective boundary conditions.

The Bubnov–Galerkin and Petrov–Galerkin method yield three Euler critical buckling loads corresponding to respective boundary conditions. Since three polynomials satisfy the mathematical model, the numerical methods estimate three critical loads of buckling alone. Here comes the interesting question of which numerical method estimates better results than analytical solutions for simply-simply supported triple-walled carbon nanotube. Table 1 to Table 3 list three critical buckling loads of triple-walled carbon nanotube for simply-simply supported boundary conditions. Among the three results like Bubnov-Galerkin-1, Bubnov-Galerkin-2, and Petrov-Galerkin-1, the Bubnov-Galerkin-2 is comparable with exact solution results. So for the triple-walled carbon nanotube with simply-simply supported boundary conditions, the Bubnov-Galerkin-2 predicts closure results reliably. From Table 4 to Table 6, it is evident that the exact solution is not listed for the clamped-clamped support of triple-walled nanotube. It is because finding the exact solutions for triple-walled nanotube with clamped-clamped support is a tough task. These three methods like Bubnov-Galerkin-1, Bubnov-Galerkin-2, and Petrov-Galerkin-1, predict reliable critical buckling loads for clamped-clamped support. Similarly, for the boundary of clamped-simply supported, Table 7 to Table 9 show the critical buckling loads. Again, Bubnov-Galerkin-1, Bubnov-Galerkin-2, and Petrov-Galerkin-1 methods estimate the critical buckling loads for triple-walled carbon nanotube with clamped-simply support in a reliable manner.

Table 1. First Euler critical buckling load P_1^E in nN, simply-simply supported TWCNT

L/D_0	10	12	14	16	18	20
B-G-1	38.832065	26.974931	19.820904	15.176341	11.991587	9.713373
B-G-2	38.375548	26.657690	19.587761	14.997816	11.850520	9.599103
P-G	38.405651	26.678608	19.603134	15.009587	11.859821	9.606637
Exact	38.326074	26.623311	19.562497	14.978470	11.835233	9.586720

Table 2. Second Euler critical buckling load P_2^E in nN, simply-simply supported TWCNT

L/D_0	10	12	14	16	18	20
B-G-1	16194.0547	23300.8321	31704.1697	41402.6500	52395.5968	64682.6542
B-G-2	16241.3171	23369.1092	31797.2302	41524.2793	52549.5883	64872.8057
P-G	16239.9778	23367.1660	31794.5769	41520.8084	52545.1919	64867.3755
Exact	16243.5254	23372.3128	31801.6045	41530.0015	52556.8364	64881.7581

Table 3. Third Euler critical buckling load P_3^E in nN, simply-simply supported TWCNT

L/D_0	10	12	14	16	18	20
B-G-1	42621.7820	61354.5922	83498.2987	109051.3209	138012.9044	170382.6518
B-G-2	42746.7303	61534.7623	83743.6729	109371.9001	138418.6983	170883.6749
P-G	42743.1726	61529.6231	83736.6684	109362.7454	138407.1079	170869.3630
Exact	42752.5958	61543.2351	83755.2208	109386.9928	138437.8066	170907.2701

Table 4. First Euler critical buckling load P_1^E in nN, clamped-clamped supported TWCNT

L/D_0	10	12	14	16	18	20
B-G-1	152.918292	106.364244	78.198875	59.890951	47.329625	38.340873
B-G-2	162.700689	113.163038	83.195627	63.717229	50.353125	40.790033
P-G	152.943073	106.372515	78.202150	59.892420	47.330349	38.341258

Table 5. Second Euler critical buckling load P_2^E in nN, clamped-clamped supported TWCNT

L/D_0	10	12	14	16	18	20
B-G-1	12262.9236	17584.8768	23892.0496	31178.7615	39442.3216	48681.3185
B-G-2	13444.5567	19281.7298	26198.9167	34190.0774	43252.3500	53384.2332
P-G	12930.5037	18546.2099	25200.5360	32887.8068	41605.3328	51351.7031

Table 6. Third Euler critical buckling load P_3^E in nN, clamped-clamped supported TWCNT

L/D_o	10	12	14	16	18	20
B-G-1	32153.9447	46219.5201	62862.0174	82075.1518	103855.9331	128202.7896
B-G-2	35257.1342	50682.8712	68934.0773	90004.0682	113889.6632	140589.1903
P-G	33912.5702	48751.9504	66308.9392	86577.2548	109553.9076	135237.3262

Table 7. First Euler critical buckling load P_1^E in nN, clamped-simply supported TWCNT

L/D_o	10	12	14	16	18	20
B-G-1	81.479486	56.624659	41.614903	31.866280	25.180343	20.397025
B-G-2	80.229103	55.760059	40.980855	31.381271	24.797308	20.086851
P-G	77.100166	53.580757	39.377714	30.153116	23.826599	19.300431

Table 8. Second Euler critical buckling load P_2^E in nN, clamped-simply supported TWCNT

L/D_o	10	12	14	16	18	20
B-G-1	14133.0340	20312.4462	27624.6933	36066.7837	45637.2936	56335.4746
B-G-2	12591.3063	18092.9441	24604.0484	32121.6703	40644.4070	50171.5212
P-G	13532.5655	19449.8759	26451.8655	34535.7039	43700.0438	53944.1772

Table 9. Third Euler critical buckling load P_3^E in nN, clamped-simply supported TWCNT

L/D_o	10	12	14	16	18	20
B-G-1	37150.7365	53453.4092	72730.5728	94978.9001	120196.8047	148383.4518
B-G-2	33090.5900	47607.4570	64773.9678	84586.8444	107044.5242	132146.1848
P-G	35573.2171	51184.1287	69643.1987	90947.2790	115094.8684	142085.1771

Fig. 1 shows the effect of L/D_o ratio over the first Euler buckling load P_1^E for three different boundary conditions of the triple-walled carbon nanotube. For the increase in the L/D_o ratio, the buckling load P_1^E decreases. It implies that for a shorter length of the nanotubes, the first critical load P_1^E is predominant compared to triple-walled nanotubes with longer lengths. This phenomenon happens in all three boundary conditions, namely clamped-clamped, clamped-simply and simply-simply supported. From Fig. 2 the second critical buckling load P_2^E increases along with L/D_o ratio increment. It happens because the Euler's critical load depends on the length of the triple-walled nanotube. But the critical buckling load P_2^E behaves entirely different from P_1^E for three different boundary conditions. The same behaviour (Fig. 3) occurs for the third Euler critical buckling load P_3^E of triple-walled carbon nanotube for simply-simply, clamped-simply, and clamped-clamped support. Fig. 4 to Fig. 6 reveal the behavior of Euler's

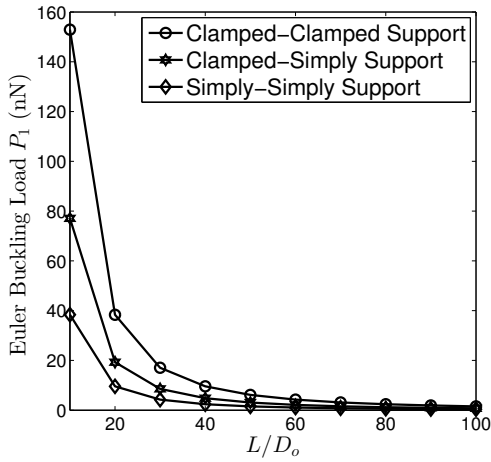


Fig. 1. Euler's first critical buckling loads for different boundary conditions vary with an aspect ratio

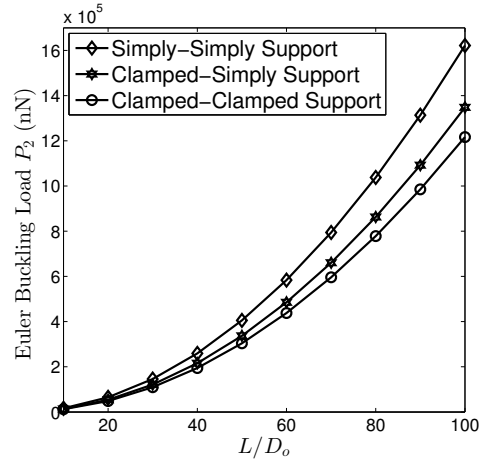


Fig. 2. Euler's second critical buckling loads for different boundary conditions vary with an aspect ratio

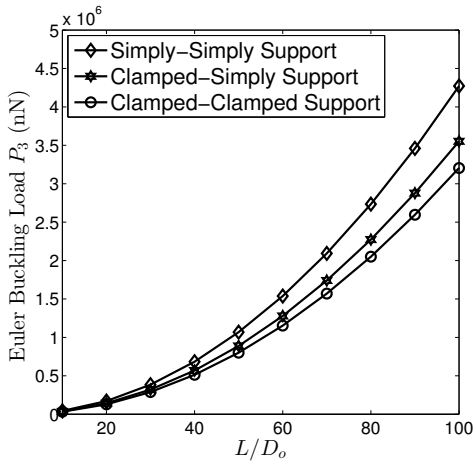


Fig. 3. Euler's third critical buckling loads for different boundary conditions vary with an aspect ratio

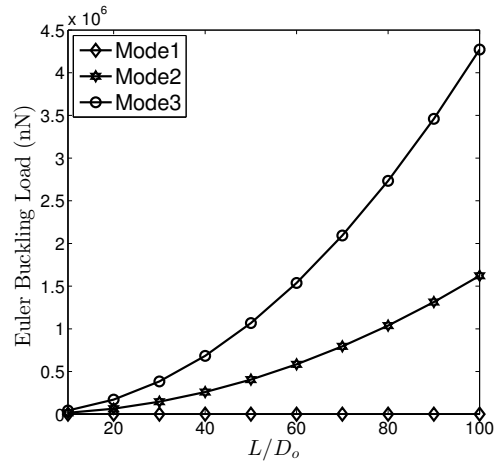


Fig. 4. First three modes of Euler's critical buckling loads for simply-simply boundary conditions vary with an aspect ratio

critical buckling load over the increase in L/D_0 ratio of the first, second, and third mode for a triple-walled carbon nanotube. The first mode interprets the fundamental buckling mode, which is the smallest buckling load among the three buckling loads. Interestingly, the fundamental Euler critical buckling mode decreases with the increase in the L/D_0 ratio. This phenomenon happens in all three boundary conditions: Simply-simply, clamped-clamped, and clamped-simply support. Further, the higher modes like second and third buckling modes increase with the increase in the L/D_0 ratio for all the

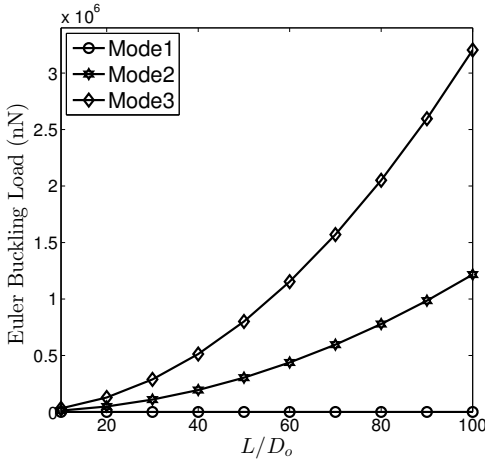


Fig. 5. First three modes of Euler's critical buckling loads for clamped-clamped boundary conditions vary with an aspect ratio

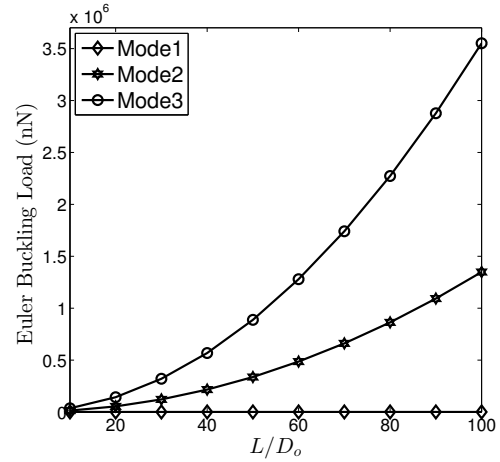


Fig. 6. First three modes of Euler's critical buckling loads for clamped-simply boundary conditions vary with an aspect ratio

boundary conditions like Simply-simply, Clamped-clamped, and Clamped-simply support. The higher modes behave entirely differently from the fundamental buckling mode for all three boundary conditions.

11. CONCLUSIONS

The present investigation estimates the Euler's critical buckling load using the mathematical model of a triple-walled carbon nanotube with a buckling effect. The Bubnov-Galerkin and Petrov-Galerkin methods determine the critical load of triple-walled nanotube quickly in a reliable manner for three different boundary conditions; namely, simply-simply, clamped-clamped, and clamped-simply supported. Two different numerical methods, namely Bubnov-Galerkin and Petrov-Galerkin method, determine the critical buckling load of triple-walled nanotube quickly in a reliable manner. For the increment of length from shorter to longer nanotube, the buckling load P_1^E decreases with the increment in length for three different boundary conditions, respectively. But the critical buckling loads of triple-walled nanotube called P_2^E and P_3^E increase for longer nanotubes in comparison with short nanotubes. So the first critical buckling load P_1^E behaves entirely different from the second and third critical buckling load, namely P_2^E and P_3^E . The two approximate methods, namely, Bubnov-Galerkin and Petrov-Galerkin method, are useful in obtaining quick and reliable results for triple-walled carbon nanotubes.

REFERENCES

- [1] S. Iijima. Helical microtubules of graphitic carbon. *Nature*, **354**, (6348), (1991), pp. 56–58. <https://doi.org/10.1038/354056a0>.

- [2] V. Senthilkumar. Axial vibration of double-walled carbon nanotubes using double-nanorod model with van der Waals force under Pasternak medium and magnetic effects. *Vietnam Journal of Mechanics*, **44**, (1), (2022), pp. 29–43. <https://doi.org/10.15625/0866-7136/16582>.
- [3] G. Dresselhaus, M. S. Dresselhaus, and R. Saito. *Physical properties of carbon nanotubes*. World Scientific, (1998).
- [4] A. Eatemadi, H. Daraee, H. Karimkhanloo, M. Kouhi, N. Zarghami, A. Akbarzadeh, M. Abasi, Y. Hanifehpour, and S. W. Sang. Carbon nanotubes: properties, synthesis, purification, and medical applications. *Nanoscale Research Letters*, **9**, (1), (2014), pp. 1–13. <https://doi.org/10.1186/1556-276X-9-393>.
- [5] C. M. Wang and C. Y. Wang. *Exact solutions for buckling of structural members*. CRC Press, (2004).
- [6] C. M. Wang, Y. Y. Zhang, Y. Xiang, and J. N. Reddy. Recent studies on buckling of carbon nanotubes. *Applied Mechanics Reviews*, **63**, (3), (2010), pp. 030804–030821. <https://doi.org/10.1115/1.4001936>.
- [7] R. C. Batra and A. Sears. Continuum models of multi-walled carbon nanotubes. *International Journal of Solids and Structures*, **44**, (22-23), (2007), pp. 7577–7596. <https://doi.org/10.1016/j.ijsolstr.2007.04.029>.
- [8] C. C. Hwang, Y. C. Wang, Q. Y. Kuo, and J. M. Lu. Molecular dynamics study of multi-walled carbon nanotubes under uniaxial loading. *Physica E: Low-dimensional Systems and Nanostructures*, **42**, (4), (2010), pp. 775–778. <https://doi.org/10.1016/j.physe.2009.10.064>.
- [9] M. Nishimura, Y. Takagi, and M. Arai. Molecular dynamics study on buckling behavior of non-defective and defective triple-walled carbon nanotubes. *Journal of Solid Mechanics and Materials Engineering*, **7**, (3), (2013), pp. 403–416. <https://doi.org/10.1299/jmmp.7.403>.
- [10] I. Elishakoff and D. Pentaras. Buckling of a double-walled carbon nanotube. *Advanced Science Letters*, **2**, (3), (2009), pp. 372–376. <https://doi.org/10.1166/asl.2009.1061>.
- [11] S. Kitipornchai, X. Q. He, and K. M. Liew. Buckling analysis of triple-walled carbon nanotubes embedded in an elastic matrix. *Journal of Applied Physics*, **97**, (11), (2005), pp. 114318–114324. <https://doi.org/10.1063/1.1925334>.
- [12] X. Guo, A. Y. T. Leung, H. Jiang, X. Q. He, and Y. Huang. Critical strain of carbon nanotubes: an atomic-scale finite element study. *Journal of Applied Mechanics*, **74**, (2), (2007), pp. 347–351. <https://doi.org/10.1115/1.2198548>.
- [13] J. Lu, C. Hwang, Q. Kuo, and Y. Wang. Mechanical buckling of multi-walled carbon nanotubes: The effects of slenderness ratio. *Physica E: Low-dimensional Systems and Nanostructures*, **40**, (5), (2008), pp. 1305–1308. <https://doi.org/10.1016/j.physe.2007.08.120>.
- [14] R. Rahmani and M. Antonov. Axial and torsional buckling analysis of single-and multi-walled carbon nanotubes: finite element comparison between armchair and zigzag types. *SN Applied Sciences*, **1**, (9), (2019), pp. 1–13. <https://doi.org/10.1007/s42452-019-1190-0>.
- [15] S. B. Coşkun. *Advances in computational stability analysis*. InTech, (2012).
- [16] D. Pentaras and I. Elishakoff. Free vibration of triple-walled carbon nanotubes. *Acta Mechanica*, **221**, (3), (2011), pp. 239–249. <https://doi.org/10.1007/s00707-011-0496-9>.
- [17] C. Q. Ru. Column buckling of multiwalled carbon nanotubes with inter-layer radial displacements. *Physical Review B*, **62**, (24), (2000), pp. 16962–16967. <https://doi.org/10.1103/PhysRevB.62.16962>.
- [18] C. Q. Ru. Effect of van der Waals forces on axial buckling of a double-walled carbon nanotube. *Journal of Applied Physics*, **87**, (10), (2000), pp. 7227–7237. <https://doi.org/10.1063/1.372973>.

- [19] C. Q. Ru. Axially compressed buckling of a doublewalled carbon nanotube embedded in an elastic medium. *Journal of the Mechanics and Physics of Solids*, **49**, (6), (2001), pp. 1265–1279. [https://doi.org/10.1016/S0022-5096\(00\)00079-X](https://doi.org/10.1016/S0022-5096(00)00079-X).
- [20] V. Senthilkumar. Buckling analysis of a single-walled carbon nanotube with nonlocal continuum elasticity by using differential transform method. *Advanced Science Letters*, **3**, (3), (2010), pp. 337–340. <https://doi.org/10.1166/asl.2010.1131>.
- [21] M. Malikan, V. A. Eremeyev, and H. M. Sedighi. Buckling analysis of a non-concentric double-walled carbon nanotube. *Acta Mechanica*, **231**, (12), (2020), pp. 5007–5020. <https://doi.org/10.1007/s00707-020-02784-7>.
- [22] I. Elishakoff, K. Dujat, G. Muscolino, S. Bucas, T. Natsuki, C. M. Wang, D. Pentaras, C. Versaci, J. Storch, N. Challamel, Y. Zhang, and G. Ghyselinck. *Carbon nanotubes and nanosensors: Vibration, buckling and ballistic impact*. John Wiley & Sons, (2013).
- [23] I. Elishakoff, K. Dujat, and M. Lemaire. Buckling of double-walled carbon nanotube. *Vietnam Journal of Mechanics*, **34**, (4), (2012), pp. 217–224. <https://doi.org/10.15625/0866-7136/34/4/2572>.
- [24] H. Shima. Buckling of carbon nanotubes: a state of the art review. *Materials*, **5**, (1), (2011), pp. 47–84. <https://doi.org/10.3390/ma5010047>.
- [25] E. Bekyarova, Y. Ni, E. B. Malarkey, V. Montana, J. L. McWilliams, R. C. Haddon, and V. Parpura. Applications of carbon nanotubes in biotechnology and biomedicine. *Journal of Biomedical Nanotechnology*, **1**, (1), (2005), pp. 3–17. <https://doi.org/10.1166/jbn.2005.004>.
- [26] L. Qin. Determination of the chiral indices (n, m) of carbon nanotubes by electron diffraction. *Physical Chemistry Chemical Physics*, **9**, (1), (2007), pp. 31–48. <https://doi.org/10.1039/b614121h>.
- [27] M. Nouredine, L. Mohamed, Y. Al-Douri, B. Djillali, and B. Mokhtar. Effect of chiral angle and chiral index on the vibration of single-walled carbon nanotubes using nonlocal Euler-Bernoulli beam model. *Computational Condensed Matter*, **30**, (2022). <https://doi.org/10.1016/j.cocom.2022.e00655>.
- [28] S. Gopalakrishnan and S. Narendar. *Wave propagation in nanostructures: Nonlocal continuum mechanics formulations*. Springer Science & Business Media, (2013).
- [29] A. Sears and R. C. Batra. Macroscopic properties of carbon nanotubes from molecular-mechanics simulations. *Physical Review B*, **69**, (23), (2004), pp. 235406–235415. <https://doi.org/https://doi.org/10.1103/PhysRevB.69.235406>.